

Channel-wise Distillation for Semantic Segmentation

Changyong Shu^{1,*} Yifan Liu^{2,*} Jianfei Gao¹, Lin Xu¹, Chunhua Shen²

¹ Shanghai Em-Data Technology Co., China

² The University of Adelaide, Australia

Abstract

Knowledge distillation (KD) has been proven to be a simple and effective tool for training compact models. Almost all KD variants for semantic segmentation align the student and teacher networks' feature maps in the spatial domain, typically by minimizing point-wise and/or pair-wise discrepancy. Observing that in semantic segmentation, some layers' feature activations of each channel tend to encode saliency of scene categories (analogue to class activation mapping), we propose to align features channel-wise between the student and teacher networks. To this end, we first transform the feature map of each channel into a distribution using softmax normalization, and then minimize the Kullback-Leibler (KL) divergence of the corresponding channels of the two networks. By doing so, our method focuses on mimicking the soft distributions of channels between networks. In particular, the KL divergence enables learning to pay more attention to the most salient regions of the channel-wise maps, presumably corresponding to the most useful signals for semantic segmentation.

Experiments demonstrate that our channel-wise distillation outperforms almost all existing spatial distillation methods for semantic segmentation considerably, and requires less computational cost during training. We consistently achieve superior performance on three benchmarks with various network structures. Code is available at: <https://git.io/ChannelDis>

1. Introduction

Semantic segmentation is a fundamental task in computer vision, which requires to assign pre-defined classes to each pixels in an input image. Its applications include autonomous driving, video surveillance, virtual reality, and so on. Thus, improving the performance of lightweight networks has drawn much attention. Effectively training lightweight networks has been studied in previous works through knowledge distillation (KD), in which, a compact network is trained with the supervision of a large teacher

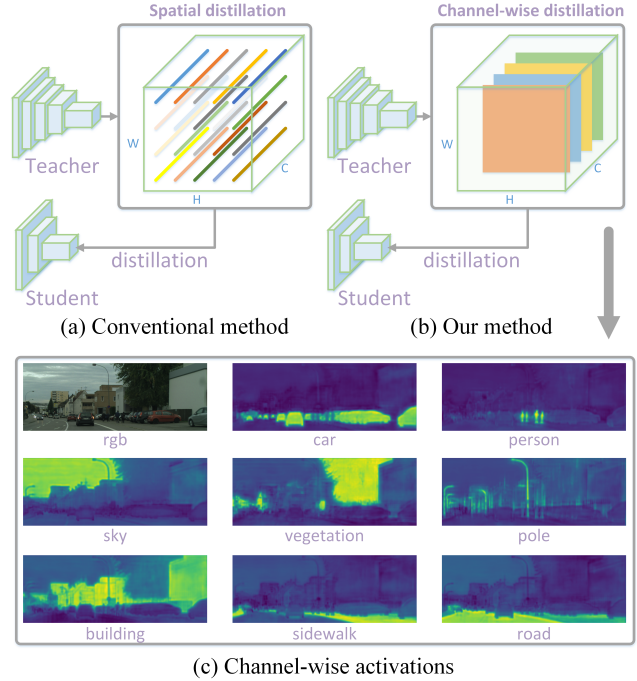


Figure 1 – Spatial knowledge distillation (top-left) works by aligning feature maps in the spatial domain. Our channel-wise distillation (top-right) instead aligns each channel of the student’s feature maps to that of the teacher network by minimizing the KL divergence. The bottom plot shows that some layers’ feature activations of each channel tend to encode saliency of scene categories.

network, and can achieve better performance. Previous works mainly focus on image classification [55, 38, 26, 3], and only a few works study KD approaches for semantic segmentation.

Semantic segmentation is a per-pixel prediction problem, which is more complex and challenging than image-level classification. Directly transferring the KD methods [27, 2] in classification to semantic segmentation may not lead to satisfactory results. Strictly aligning the point-wise classification scores or the feature activations between the teacher network and the compact student network may enforce overly strict constraints and can lead to sub-optimal solutions.

*First two authors contributed equally.

Recent works [37, 36, 30] pay attention to enforce the correlations among different spatial locations, namely structural knowledge distillation. As shown in Figure 1(a), let y^T and y^S be the feature maps (or the score maps) from the teacher network and student network, respectively. Then the original knowledge distillation function φ , can be formulated as: $\varphi(y^T, y^S) = \varphi(\phi(y_i^T), \phi(y_i^S))$, where $\phi(\cdot)$ is some transformations applied to the features, typically being nonlinear; and i indicates the pixel index. $y_i^T \in \mathbb{R}^C$ and $y_i^S \in \mathbb{R}^C$ are vectors for a spatial location. C is the number of channels. Such methods may work better than the point-wise alignment in capturing spatial structure information, and improve the performance of the student network. Almost all previous methods, referred to as spatial distillation, take the activation vectors along the channel axis at one spatial location as the feature vectors, either for point-wise or pair-wise correlation alignment. We argue that such a requirement may be overly harsh. Usually the teacher network’s feature maps contain redundant and possibly noisy information which may not contribute to the final prediction. It is better that KD can transfer the useful signals to the student network while discarding the noises in the feature maps.

To alleviate those limitations, here we propose a novel channel-wise distillation paradigm for semantic segmentation from a new perspective. Inspired by the observation in Figure 1(c), the feature activations of each channel tend to encode saliency of scene categories of an input image. When learning using knowledge distillation, the compact network is expected to focus more on the salient activations associated to the semantic parts, rather than other regions which may be the background or noises of a specific channel. We want to transfer the informative regions at each channel of the teacher network’s feature maps to the student network. To do so, we first transfer the activations of each channel into a distribution by using the softmax normalization. Similar to the original KD, we employ the KL divergence to minimize the discrepancy between channel-wise activation distributions of the teacher network and the student network.

To summarize, we propose the efficient and effective channel-wise distillation paradigm for segmentation segmentation, where the discrepancy of the channel-wise activation distributions between the teacher and student network is minimized for each channel individually. As shown in Figure 1(b), the channel-wise distillation loss can be formulated as: $\varphi(y^T, y^S) = \varphi(\phi(y_c^T), \phi(y_c^S))$, where c indicates the channel index. y_c^T and y_c^S are the activations for each channel with the spatial size of $W \times H$. The main contributions can be summarized as follows:

- Unlike those existing spatial distillation approaches, we propose a novel channel-wise distillation paradigm for knowledge distillation for semantic segmentation.

- The proposed channel-wise distillation significantly outperforms seven state-of-the-art KD methods for semantic segmentation and requires less computational cost during training.
- We show consistent improvements on a few benchmark datasets with various network structures, demonstrating that our method is general. Given its simplicity and effectiveness, we believe that our method can serve as a strong baseline KD method for semantic segmentation.

1.1. Related Work

Early works on knowledge distillation focus on classification tasks [27, 5, 39, 48, 50, 49, 20, 56, 21], and it has been extended to other tasks such as semantic segmentation [24, 15, 36, 30], object detection [42, 9, 17, 29], re-identification [6, 46, 4], face recognition[31], style transfer [14], GAN [11, 33] and so on.

Our work aims to study efficient and effective distillation methods for semantic segmentation, beyond naively applying pixel-wise distillation as done in classification. Previous methods usually align spatial structure information among pixels. The feature map of the student network is forced to be similar to that of the teacher network via L_2 loss [15]. In [47], a local similarity map is constructed to minimize the discrepancy of segmented boundary information between the teacher and student network, where the euclidean distance among the center pixel and the 8-neighborhood pixels is used as knowledge for transferring. Liu *et al.* [36] first propose the concept of structure knowledge distillation. They propose two approaches to capture the structure information among pixels, including pair-wise similarity between pixels and holistic correlations captured by a discriminator. As the pixels far apart usually exhibit low similarity, the connection range and the granularity of each node in pairwise loss are further studied in [37]. The work in [45] only focuses on the intra-class feature variation among the pixels with same label, where the set of cosine distance between each pixel’s feature and its corresponding class-wise prototype is constructed to transfer the structural knowledge. Besides, an auto-encoder is used to compress features [24], and the feature adaptor is employed to mitigate the feature mismatching between the teacher and student networks.

All these methods consider the N channel activation values of a spatial location as the feature vectors to operate on. Here, we take a different route and perform channel-wise KD.

A recent independent work [61] also pays attention to the knowledge lying in each channel. Zhou *et al.* calculate the mean of the activation in each channel, and align a weighted difference for each channel in classification. Therefore, a class-independent correlation are encoded. Different from

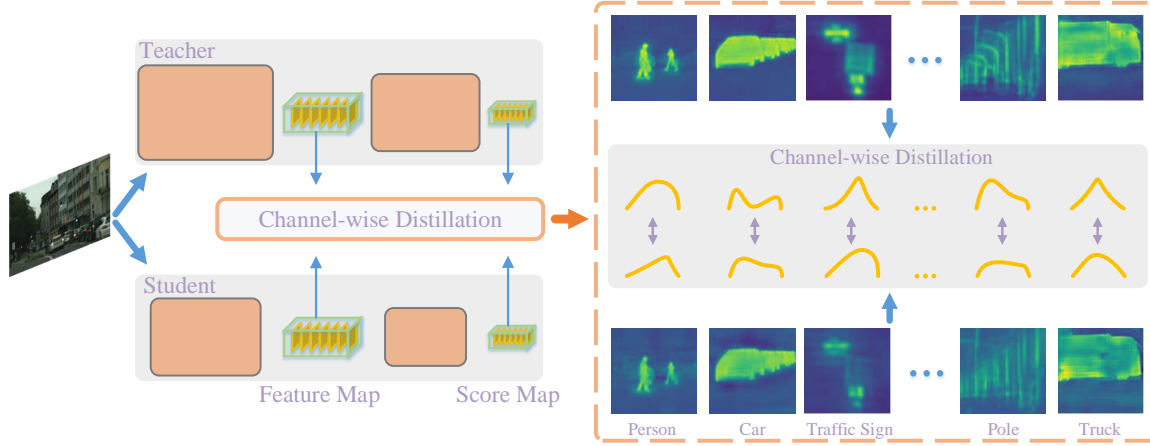


Figure 2 – The overall architecture of our proposed method. The plot on the left is the paradigm of our teacher-student strategy, where the feature map and the score map are used for channel-wise distillation. The plot on the right is the detailed description of channel-wise distillation. Activated regions correspond to scene categories.

[61], we perform channel-wise distillation for semantic segmentation. Our work aligns the distributions of each channel, which guides the student network to learn the informative/salient locations of the activation maps.

2. Method

In this section, we first present a brief introduction to spatial knowledge distillation, and then we describe our proposed channel-wise distillation.

2.1. Spatial Distillation

Existing KD methods often employ a point-wise alignment or align structured information among spatial locations, which can be formulated as:

$$\ell = \ell_{ce}(y, y^S) + \alpha \cdot \varphi(\phi(y_i^T), \phi(y_i^S)). \quad (1)$$

Here the cross-entropy loss ℓ_{ce} is still applied for semantic segmentation with y being the ground-truth labels. α is a hyper-parameter. For better illustrating the knowledge distillation functions $\varphi(\cdot)$ and the transformation $\phi(\cdot)$ used in the literature, representative spatial distillation methods are listed in Table 1. MIMIC transfers the feature of each pixel via L_2 loss [2, 34]. Attention Transfer (AT) [53] uses an attention mask to squeeze the feature maps into a single channel for distillation. The pixel-wise loss [28] directly aligns the point-wise class probabilities. The local affinity [47] is computed by the distance between the center pixel and its 8 neighborhood pixels. The pairwise affinity [37, 24, 36] is employed to transfer the similarity between pixel pairs. The similarity between each pixel’s feature and its corresponding class-wise prototype is computed to transfer the structural knowledge [45]. The holistic loss [37, 36] use the

adversarial scheme to align the high-order relations between feature maps from the two networks. Note that, the last four terms consider the correlation among pixels. Existing KD methods as shown in Table 1 are all spatial distillation methods.

2.2. Channel-wise Distillation

Inspired by Figure 1(c), the activation of different channels encodes the saliency of scene categories of an input image. Besides, a well-trained teacher network tends to produce activation maps of clearer category-specific masks for each channel—which is expected—as illustrated on the right part of Figure 2. We propose a novel channel-wise distillation paradigm to guide the student to directly learn the channel-wise distribution from the well-trained teacher.

As illustrated in Figure 2, our method consists of the teacher network, student network, and channel-wise distillation module. The teacher and student network are denoted as T and S , and the activation maps from T and S are y^T and y^S , respectively. The channel-wise distillation loss can be formulated as:

$$\varphi(\phi(y^T), \phi(y^S)) = \varphi(\phi(y_c^T), \phi(y_c^S)). \quad (2)$$

Here, we give a simple but effective scheme for ϕ and φ in Equation (2). First, we apply a softmax normalization to transfer the activation values in each channel into a distribution ϕ_{cw} :

$$\phi_{cw}(y_c) = \frac{\exp(\frac{y_{c,i}}{\mathcal{T}})}{\sum_{i=1}^{W \cdot H} \exp(\frac{y_{c,i}}{\mathcal{T}})}, \quad (3)$$

where $c = 1, \dots, C$. C is the number of channels and \mathcal{T} is the temperature. The distribution will be softer if we use

Loss	$\varphi(u, v)$	$\phi(x)$	
		Formulation	Dimensionality
Point-wise alignment			
Mimic [2, 34]	L_1 or L_2	x_i	$C \times W \times H$
Attention transfer [53]	L_1 or L_2	$\sum_{c=1}^C \ x_{ic}\ ^p$	$1 \times W \times H$
Pixelwise [37, 13, 36, 45]	KL	$\text{softmax}(x_i/\tau)$	$C \times W \times H$
Pairwise or higher order alignment			
Local similarity [47]	L_1 or L_2	$\sum_{j \in N(i)} \ x_j - x_i\ $	$1 \times W \times H$
Pairwise affinity [37, 24, 36]	L_2	$\frac{x_i^T x_j}{\ x_i\ _2 \cdot \ x_j\ _2}$	$1 \times W \times H$
IFVD [45]	L_2	$\cos(x_i, \sum_{j \in S_i} x_j / S_i)$	$1 \times W \times H$
Holistic [37, 36, 45]	Wasserstein Distance	$D(x_i)$	1

Table 1 – Current spatial distillation methods. i and j indicates the pixel index. $D(\cdot)$ is a discriminator, and $N(i)$ indicates 8-neighborhood of pixel i . S_i is the pixel set having the same label as pixel i and $|S_i|$ stands for the size of the set S_i .

a larger \mathcal{T} , which means we focus on more regions in each channel. By applying the softmax normalization, we remove the influences of different magnitude scales between the large networks and the compact networks, which will benefit the knowledge distillation as shown in the previous work [43]. A 1×1 convolution layer will be employed to upsampling the number of channels for the student network if the number of channels is different between the teacher and the student. The spatial locations with higher probability are the most salient regions, presumably corresponding to the most useful signals for semantic segmentation.

We use the KL divergence to minimize the discrepancy of the channel-wise distribution between the teacher and student network, and the knowledge distillation function φ_{cw} , can be formulated as:

$$\varphi_{cw}(y^T, y^S) = \sum_{c=1}^C \sum_{i=1}^{W \cdot H} \phi(y_{c,i}^T) \cdot \log \left[\frac{\phi(y_{c,i}^T)}{\phi(y_{c,i}^S)} \right]. \quad (4)$$

The KL divergence is an asymmetric metric. From Equation (4), we can see if $\phi(y_{c,i}^T)$ is large, the $\phi(y_{c,i}^S)$ should be as large as $\phi(y_{c,i}^T)$ to minimize the KL divergence; otherwise, if $\phi(y_{c,i}^T)$ is very small, the KL divergence will pay less attention to minimize the $\phi(y_{c,i}^S)$. Thus, the student network tend to produce similar activation distribution in the foreground scenery parts and ignore the redundancy background.

2.3. Optimization

To train our network, we define a loss function in Equation (5) including two terms: a multi-label cross entropy loss ℓ_{ce} , and the channel-wise distillation loss φ_{cw} :

$$\ell = \ell_{ce}(y, y^S) + \alpha \cdot \varphi_{cw}(y^T, y^S), \quad (5)$$

where α is a balance hyper-parameter and we set to 35 in all of our experiments. Following other distillation frameworks, we employ a well-trained large network as our

teacher net and fix the weight of the teacher during the training phase. We only optimize the parameters of the student network during the training phase.

3. Experiments

In this section, we first describe the implementation details and conduct ablation studies. Then, we compare our channel-wise distillation method with other state-of-the-art distillation methods. Finally, we show consistent improvements in different typical semantic segmentation datasets and student network structures.

3.1. Experimental Settings

Datasets. Three representative semantic segmentation benchmarks, *i.e.*, Cityscapes [16], ADE20K [60] and Pascal VOC [19] are considered. The Cityscapes dataset is used for semantic urban scene understanding. It contains 5,000 finely annotated images with 2,975/500/1,525 images for training/validation/testing respectively, where 30 common classes are provided and 19 classes are used for evaluation and testing. The size of each image is 2048×1024 pixels. And there are all gathered from 50 different cities. The coarsely labeled data is not used in our experiments.

The Pascal VOC dataset contains 1,464/1,449/1,456 images for training/validation/testing. It contains 20 foreground objects classes and an extra background class. In addition, the dataset is augmented by extra coarse labeling, which resulting in 10,582 images for training. The training split is used for training, and the final performance is measured on the validation set across 21 classes.

The ADE20K dataset covers 150 classes of diverse scenes, where the annotation is detailed for semantic parsing. It contains 20K/2K/3K images for training, validation, and testing. In our experiments, we report the segmentation accuracy on the validation set.

Evaluation Metrics. To evaluate the performance and efficiency of our proposed channel-wise distillation method, we test each strategy via the mean Intersection-over-Union

Network			Structural	Complexity	Val mIoU(%)	
					Featuremap	Scoremap
Teacher			—	—	78.56	78.56
Student			—	—	69.10	69.10
Individual Competition	Spatial Distillation	MIMIC [2, 34]	×	$h_x \cdot w_x \cdot c_x$	72.21(+3.45) [⊗]	72.10(+3.00)
		AT [53]	×	$h_x \cdot w_x \cdot (c_x)^p$	72.37(+3.27) [⊗]	72.32(+3.22)
		PI [13, 45, 37, 36]	×	$h_x \cdot w_x \cdot c_x$	70.02(+0.92) [⊗]	71.74(+2.64)
		LOCAL [47]	✓	$8h_x \cdot w_x \cdot c_x$	69.81(+0.71)	69.75(+0.65)
		PA [37, 24, 36]	✓	$(h_x \cdot w_x)^2 \cdot c_x$	71.23(+2.13)	71.41(+2.31)
		IFVD [45]	✓	$h_x \cdot w_x \cdot c_x \cdot n$	71.35(+2.25)	70.66(+1.56)
		HO [37, 36, 45]	✓	$\mathcal{O}(D)$	— [⊗]	72.13(+3.03)
	Channel-wise Distillation	CW (Ours)	✓	$h_x \cdot w_x \cdot c_x$	73.52(+4.42)[⊗]	72.82(+3.72)

Table 2 – Comparison between computation complexity and performance on the validation set among different individual distillation methods. The mIoU is calculated on the Cityscapes validation set with PSPNet-R101 as the teacher network and PSPNet-R18 as the student network. The complexity depends on the shape $(h_x \times w_x \times c_x)$ of the input, which can be the score map or the feature map. $\mathcal{O}(D)$ denotes the discriminator complexity. The superscript [⊗] means that additional channel alignment convolution is needed.

(mIoU) to indicate the segmentation accuracy in all experiments under a single-scale setting. Besides, the mean class Accuracy (mAcc) is listed for Pascal VOC and ADE20K. The parameter number is computed by summing the parameters in the model and the floating-point operations per second (FLOPs) are calculated with a fixed input size (512×1024).

Implementation Details. The teacher network is PSPNet with ResNet101 (PSPNet-R101) as the backbone for all experiments. We employ several different architectures, including PSPNet, Deeplab with the backbones of ResNet18, and MobileNetV2 as student networks to verify the effectiveness of the channel-wise distillation. In the ablation study, we analyze the effectiveness of our method based on PSPNet with ResNet18 (PSPNet-R18). Unless otherwise indicated, the training image for the student is randomly cropped into 512×512 , the batch size is set to 8, and the number of the training step is 40k.

3.2. Ablation study

We discuss the choice of the hyper-parameters and the effect of the asymmetric KL divergence in this section. The baseline student model is PSPNet-R18, and the teacher model is the PSPNet-R101. All the results are evaluated on the validation set of Cityscapes.

Impact of the temperature parameter. We conduct experiments to change the channel-wise distribution by adjusting the temperature parameter \mathcal{T} . The results are shown in Figure 3. The loss weight is set to 35, and $\mathcal{T} \in [0.01, 1000]$. The distribution tends to be softer if we increase \mathcal{T} , which means we focus on more regions. We get the best performance when $\mathcal{T} = 1$. Besides, in a certain range, the performance is stable. The performance will drop a lot if \mathcal{T} is extremely small, which means we only focus on limited salient pixels.

Impact of the loss weight. The experiment results of adjusting the loss weight are shown in Figure 3. We fix $\mathcal{T} = 1$,

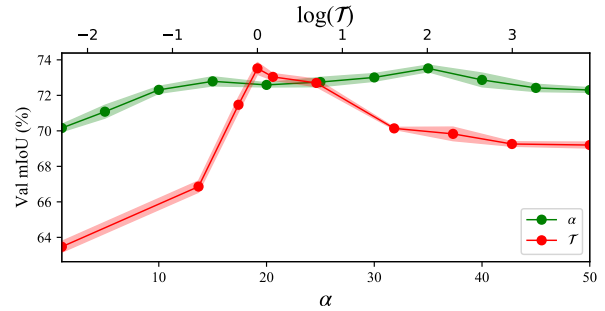


Figure 3 – Impact of the temperature parameter \mathcal{T} and the loss weight α .

and adjust the loss weight in $[0, 50]$. We can see that the distillation results are not sensitive to the loss weight. We set $\alpha = 35$ in all experiments.

Impact of the distribution metric. The channel-wise distribution and asymmetric KL divergence play an important role in our distillation method. We conduct experiments with three different metrics to show the effectiveness of proposed methods in Table 3. The Bhattacharyya distance [7] is a symmetric distribution measurement, which aligns the discrepancy in each channel. The L_2 norm considers the difference at all locations in all channels equally, which is similar to the previous MIMIC method. From Table 3, we can see that the asymmetric KL divergence considering the channel-wise discrepancy achieves the best performance. Note that as the KL divergence is asymmetric, the input of the student and teacher can not be swapped. We conduct the experiment by changing the order of the input in the KL divergence, and the training does not converge.

3.3. Comparison with Spatial Distillation

In this subsection, we first analyze the individual comparison of previous state-of-the-art spatial distillation methods, then study the benefits of combining with previous spa-

Metric	Baseline	KL	Bhat. [7]	L_2
mIoU (%)	69.10	73.52	72.21	71.60

Table 3 – The effect of the distribution metric. Bhat. is short for the Bhattacharyya distance. The asymmetric KL divergence achieves the best performance.

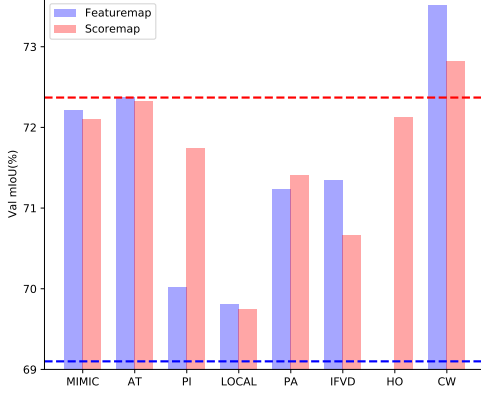
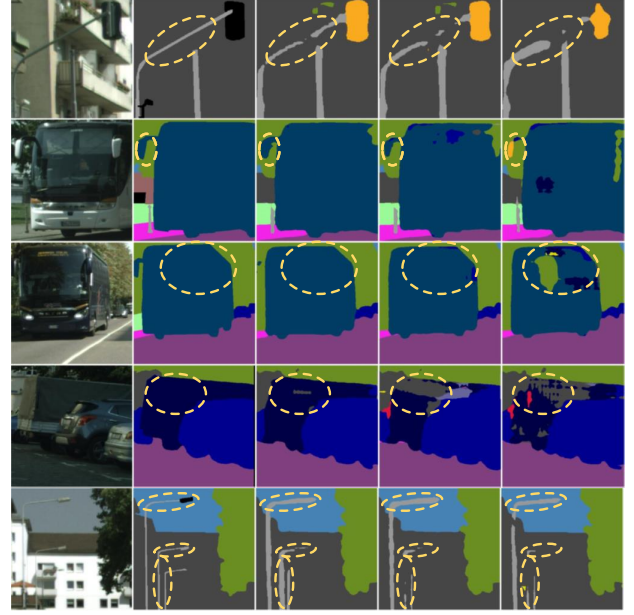


Figure 4 – Illustration of the performance under different individual distillation methods. The red (blue) dotted line is the performance of AT (student). The proposed channel-wise distillation method achieves better results than any other spatial distillation methods.

tial distillation methods.

Individual comparison. To verify the effectiveness of our proposed channel-wise distillation, we compare our method with current spatial distillation methods listed below:

- MIMIC: Transfer the feature of each pixel via L_2 loss [2, 34].
- Squeeze attention transfer for distillation (AT): Sergey [53] utilizes attention transfer to squeeze an attention map to distill.
- Local affinity study (LOCAL): For each pixel, a local similarity map is constructed, which consider the correlations between itself and its 8 neighborhood pixels [47].
- Pixelwise logits distillation (PI): KL divergence is used to align the predicted logits for each pixel [37, 36, 45, 13].
- Pairwise relation distillation (PA): The correlations between each pixel pair are considered [37, 24, 36].
- Intra-class feature variation distillation (IFVD): The set of similarity between the feature of each pixel and its corresponding class-wise prototype is regarded as the intra-class feature variation to transfer the structural knowledge [45].
- Holistic distillation (HO): The holistic embeddings of feature maps are computed by a discriminator, which are used to minimize the discrepancy between high-order relations [37, 36, 45].



(a) Image (b) GT (c) CW (d) AT (e) Student

Figure 5 – Qualitative segmentation results on Cityscapes produced from PSPNet-R18: (a) raw images, (b) ground truth (GT), (c) channel-wise distillation (CW), (d) the best spatial distillation schemes: attention transfer (AT), and (e) output of the original student model.

The conventional multi-class cross-entropy loss is applied in all experiments. The computational complexity and performance of different spatial distillation methods are studied. Given the input feature map (score map) with the size of $h_f \times w_f \times c$ ($h_s \times w_s \times n$), where h_f (h_s) \times w_f (w_s) is the shape of the feature map (score map). c is the number of channels and n is the number of classes. As shown in Table 2, all distillation methods can improve the performance of the student network. Our channel-wise distillation method outperforms all spatial distillation methods, it outperforms the best spatial distillation method (AT) by 1.15%. Moreover, channel-wise distillation is very efficient as it requires less computational cost than other methods during the training phase. The Mimic has the same complexity as our proposed method, but the performance is lower than the proposed channel-wise distillation. The channel-wise distillation on the feature map works better than on the score map, which may due to that the channel number is larger on the feature map and may contain more detailed salient objects. To better show the improvement, we illustrate the results of Table 2 in Figure 4.

The attention transfer [53] squeezes all the channels into a single channel attention map (e.g., find the max activation or the summation). On the contrary, the channel-wise distillation aligns the distribution in each channel (remove the influences of magnitude scales) and then calculates the difference in all channels.

Method	mIoU	road	sidewalk	building	wall	fence	pole	traffic light	traffic sign	vegetation
PA	71.41	97.30	80.48	90.76	37.89	52.78	60.33	63.48	74.06	91.69
IFVD	71.66	97.56	81.44	91.49	44.45	55.95	62.40	66.38	76.44	91.85
CW	73.60	97.65	82.25	91.43	46.54	55.62	62.57	68.48	76.74	91.99
Class	terrain	sky	person	rider	car	truck	bus	train	motorcycle	bicycle
PA	58.60	93.48	78.96	55.45	93.42	63.79	78.48	60.12	51.62	74.01
IFVD	61.29	93.97	78.64	52.33	93.50	60.25	74.70	58.81	44.85	75.41
CW	62.28	93.99	79.77	55.84	94.12	64.73	84.73	64.80	48.62	76.17

Table 4 – The class IoU of our proposed channel-wise distillation method compared with the other two typical structural knowledge transfer methods on the validation set of Cityscape, where PSPNet-R18 (1.0) was selected as the student network.

Network			Complexity	Val mIoU(%)	Test mIoU(%)
Teacher			–	78.53	76.78
Student			–	69.10	67.60
Combinations	Spatial Distillation	PI+HO	$h_s w_s n + O(D)$	72.77(+3.67)	–
		PI+HO+PA _f	$h_s w_s n + O(D) + h_f^2 w_f^2 c$	74.08(+4.98)	–
		PI+HO+IFV _f	$h_s w_s n + O(D) + h_f w_f c n$	74.54(+5.44)	72.74(+5.10)
	Channel-wise(Ours)	CW _s +CW _f	$h_f w_f c + h_s w_s n$	73.71(+4.61)	–
	Spatial Distillation+ Channel-wise(Ours)	PI+HO+CW _f PI+HO+CW _s +CW _f	$h_s w_s n + O(D) + h_f w_f n$ $h_s w_s n + O(D) + h_f w_f n + h_s w_s c$	74.87(+5.77) 75.13(+6.03)	73.86(+6.26) 74.18(+6.58)

Table 5 – Performance under different combinations. The PI and HO are both used to transfer the knowledge encoded in the score map and employed as base components in all methods.

To demonstrate the effectiveness, we compare our method with current state-of-the-art spatial distillation methods, including PA and IFVD. These methods propose to transfer structure information in semantic segmentation. We list the detailed class IoU of three methods in Table 4. Our methods significantly improve the class accuracy of several objects, such as traffic light, terrain, wall, truck, bus, and train, indicating that the channel-wise alignment can transfer the structural knowledge better.

We also present the visualization results in Figure 5 to intuitively demonstrate that, the channel-wise distillation method (CW) outperforms the spatial distillation strategy. Moreover, to evaluate the effectiveness of the proposed channel-wise distillation, we visualize the channel-wise distribution of the student network under three paradigms, *i.e.*, original network, distilled result by attention transfer (AT) and channel-wise distillation respectively, in Figure 6.

Impact of combinations. We evaluate the performance under a few different loss combinations, as shown in Table 5. First we combine the channel-wise distillation applying to the feature map and the score map. The results can be improved to 73.71%. Current state-of-the-art methods [37, 30] combine the pixel-wise distillation (PI), the holistic distillation (HO) on the score map and PA/IFVD on the feature map for further improving the performance. To make a fair comparison, we also combine the proposed channel-wise distillation with PI and HO on the score map. As shown in Table 5, we can see that the proposed channel-wise distillation method is not contradicted to previous spatial distillation methods and outperforms the state-of-the-art distillation methods [30, 37] when combining with previous spatial

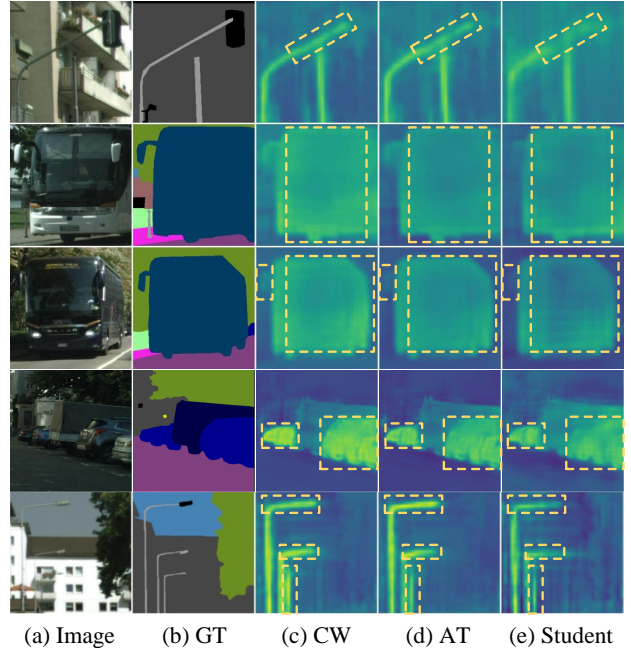


Figure 6 – The channel-wise distribution of the student under three paradigms. The yellow dotted lines show the activation maps of CW are better than that in AT and the student network.

distillation methods.

3.4. Results

We demonstrate that our proposed method can bring consistent improvement compared to state-of-the-art semantic

segmentation distillation methods, *i.e.*, structural knowledge distillation for segmentation/dense prediction (SKDS [36] /SKDD [37]) and intra-class feature variation distillation (IFVD [45]), under various student networks.

Cityscapes. We first evaluate the performance of our method on the Cityscapes dataset. As the SKDS/SKDD (IFVD) take $PI+HO+PA_f$ ($PI+HO+IFVD_f$) in their methods, for a fair comparison, we also employ PI and HO in our method. Various student networks with different encoders and decoders are used to verify the effectiveness of our method. Encoders include ResNet18 (initialized with or without the weights pre-trained on ImageNet, a channel-halved variant of ResNet18 [23]) and MobileNetV2 [41], and decoders include PSPhead [59] and ASPPhead [12]. Table 6 summarizes our method’s performance applied for different student models on Cityscapes. Experiment results on Pascal VOC and ADE20K are shown in the supplementary materials).

Our method outperforms SKD and IFVD on seven student networks, which further indicates that the channel-wise distillation is effective for semantic segmentation distillation and can complement the spatial distillation.

For the student with the same architectural type as the teacher, *i.e.*, PSPNet-R18 $^\diamond$ (0.5), PSPNet-R18 $^\diamond$ and PSPNet-R18*, the improvement is more significant. As for the student with different architectural types with the teacher, *i.e.*, PSPNet-MBV2*, Deeplab-R18 $^\diamond$ (0.5), Deeplab-R18* and Deeplab-MBV2*, our method achieves consistent improvement compared with SKDS and IFVD, which proves that our channel-wise distillation is more effective and can generalize well between different teacher and student networks.

The student network of a compact model capacity (PSPNet-R18 $^\diamond$ (0.5)) shows inferior distillation performance (67.26%) compared to the student with large parameters (PSPNet-R18*) (74.87%). This may be attributed to the fact that the capability of small networks is limited compared with the teacher network and can not sufficiently absorb the knowledge of the current task. For PSPNet-R18, the student initialized by the weight trained on ImageNet obtains the best distillation performance (improved from 70.04% to 74.87%), further demonstrating that the well-initialized parameters help the distillation. Thus, the better student lead to better distillation performance, but the improvement is smaller as the gap between the teacher and student network is smaller.

4. Conclusion

In this paper, we have summarized previous segmentation distillation methods as the spatial distillation paradigm, and a novel structural knowledge transfer strategy, *i.e.*, channel-wise distillation, is proposed. Experimental results show that the proposed channel-wise distillation method

Method	Params (M)	FLOPs (G)	mIoU (%)	
			Val	Test
ENet [11]	0.358	3.612	—	58.3
ESPNet [40]	0.363	4.422	—	60.3
ERFNet [18]	2.067	25.60	—	68.0
ICNet [57]	26.50	28.30	—	69.5
FCN [32]	134.5	333.9	—	62.7
RefineNet [35]	118.1	525.7	—	73.6
OCNet [52]	70.43	574.9	—	78.4
Results w/ and w/o distillation schemes				
T:PSPNet [59]	70.43	574.9	78.5	78.4
S:PSPNet-R18 $^\diamond$ (0.5)	3.835	31.53	55.40	54.10
+SKDS [36]	3.835	31.53	61.60	60.50
+SKDD [37]	3.835	31.53	62.35	—
+IFVD [45]	3.835	31.53	63.35	63.68
+Ours	3.835	31.53	67.26	67.33
S:PSPNet-R18 $^\diamond$	13.07	125.8	57.50	56.00
+SKDS [36]	13.07	125.8	63.20	62.10
+SKDD [37]	13.07	125.8	64.68	—
+IFVD [45]	13.07	125.8	66.63	65.72
Ours	13.07	125.8	70.04	70.11
S:PSPNet-R18*	13.07	125.8	69.72	67.60
+SKDS [36]	13.07	125.8	72.70	71.40
+SKDD [37]	13.07	125.8	74.08	—
+IFVD [45]	13.07	125.8	74.54	72.74
+Ours	13.07	125.8	74.87	73.86
S:PSPNet-MBV2*	1.98	16.40	58.64	57.43
+SKDS [36]	1.98	16.40	61.12	60.36
+IFVD [45]	1.98	16.40	62.74	61.92
+Ours	1.98	16.40	64.37	63.12
S:Deeplab-R18 $^\diamond$ (0.5)	3.15	31.06	61.83	60.51
+SKDS [36]	3.15	31.06	62.71	61.69
+IFVD [45]	3.15	31.06	63.12	62.37
+Ours	3.15	31.06	65.60	64.33
S:Deeplab-R18*	12.62	123.9	73.37	72.39
+SKDS [36]	12.62	123.9	73.87	72.63
+IFVD [45]	12.62	123.9	74.09	72.97
+Ours	12.62	123.9	75.25	74.12
S:Deeplab-MBV2*	2.45	20.39	65.94	65.07
+SKDS [36]	2.45	20.39	66.73	65.81
+IFVD [45]	2.45	20.39	67.04	66.12
+Ours	2.45	20.39	67.92	66.87

Table 6 – Comparison of student variants with the state-of-the-art distillation methods on Cityscapes, where $^\diamond$ denotes to be trained from scratch and * indicates to be initialized by the weights pre-trained on ImageNet, and R18 (MBV2) is the abbreviation for Resnet18 (MobileNetV2).

consistently outperforms almost all existing KD methods on three public benchmark datasets with various network backbones. Additionally, our experiments demonstrate the efficiency and effectiveness of our channel-wise distillation, and it can further complement the spatial distillation methods. We hope that the proposed simple and effective channel-wise distillation can serve as a strong baseline for effectively training compact networks for many other dense prediction tasks, including object detection, instance segmentation and panoptic segmentation.

A. Additional results

S2. Results on Pascal VOC and ADE20K

In order to compare the essential contribution of different methods, we dismantle the PI and HO in SKDS and IFVD, and the experiments are conducted on Pascal VOC and ADE20K. Multi student-network variants with different encoders and decoders are used to validate the efficiency of our method. Here, encoders include ResNet18 and MobileNetV2, and decoders include PSP-head and ASPP-head.

Method	Params	mIoU(%)	mAcc(%)
FCN [32]	134.5	69.9	78.1
DeepLabV3 [12]	87.1	77.9	85.7
PSANet [58]	78.13	77.9	86.6
GCNet [8]	68.82	77.8	85.9
ANN [62]	65.2	76.7	84.5
OCRNet [51]	70.37	80.3	87.1
Results w/ and w/o our distillation schemes			
T:PSPNet [59]	70.43	78.52	79.57
S:PSPNet-R18	13.07	65.42	80.43
+SKDS [36]	13.07	67.73	81.73
+IFDV [45]	13.07	68.04	82.25
+Ours	13.07	69.25	83.14
S:PSPNet-MBV2	1.98	62.38	77.82
+SKDS [36]	1.98	63.95	78.93
+IFDV [45]	1.98	64.73	79.81
+Ours	1.98	65.93	81.45
S:Deeplab-R18	12.62	66.81	81.14
+SKDS [36]	12.62	68.13	82.26
+IFDV [45]	12.62	68.42	82.70
+Ours	12.62	69.97	83.47
S:Deeplab-MBV2	2.45	50.80	74.24
+SKDS [36]	2.45	52.11	75.17
+IFDV [45]	2.45	53.39	76.02
+Ours	2.45	54.62	77.13

Table 7 – mIoU and mAcc on validation set of VOC 2012, R18 (MBV2) is the abbreviation for Resnet18 (MobileNetV2).

Pascal VOC. We evaluate the performance of our method on the Pascal VOC dataset. The distillation results are listed in Table 7. Our proposed CW improves PSPNet-R18 without distillation by 3.83%, outperforms the SKDS and IFVD by 1.51% and 1.21%. Consistent improvements on other student networks with different encoders and decoders are achieved. The gains on PSPNet-MBV2 with our method is 3.55%, surpassing the SKDS and IFVD by 1.98% and 1.20%. As for Deeplab-R18, our CW improves the student from 66.81% to 69.97%, outperforming the SKDS and IFVD by 1.84% and 1.55% respectively. Besides, the performance of Deeplab-MBV2 with our distillation is increased from 50.80% to 54.62%, outperforming the SKDS

Method	Params	mIoU(%)	mAcc(%)
FCN [32]	134.5	39.91	49.62
DeepLabV3 [12]	87.1	44.99	55.81
PSANet [58]	78.13	43.74	54.09
GCNet [8]	68.82	43.68	54.28
ANN [62]	65.2	42.93	53.25
OCRNet [51]	70.37	43.70	53.74
Results w/ and w/o our distillation schemes			
T:PSPNet [59]	70.43	44.39	45.35
S:PSPNet-R18	13.07	24.65	33.66
+SKDS [36]	13.07	25.11	33.72
+IFDV [45]	13.07	25.72	33.83
+Ours	13.07	26.80	34.02
S:PSPNet-MBV2	1.98	23.15	32.93
+SKDS [36]	1.98	24.79	34.04
+IFDV [45]	1.98	25.33	35.57
+Ours	1.98	27.97	37.16
S:Deeplab-R18	12.62	24.89	33.60
+SKDS [36]	12.62	25.52	34.10
+IFDV [45]	12.62	26.53	34.79
+Ours	12.62	27.37	35.34
S:Deeplab-MBV2	2.45	24.98	35.34
+SKDS [36]	2.45	26.10	36.51
+IFDV [45]	2.45	27.25	37.23
+Ours	2.45	29.18	38.08

Table 8 – mIoU and mAcc on validation set of ADE20K, R18 (MBV2) is the abbreviation for Resnet18 (MobileNetV2).

and IFVD by 2.51% and 1.23% respectively.

ADE20K. We also evaluate our method on the ADE20K dataset to further demonstrate that CW works better than other structural knowledge distillation methods. The results are shown in Table 8. Our proposed CW improves PSPNet-R18 without distillation by 3.83%, and outperforms the SKDS and IFVD by 1.51% and 1.21% in several. Notable performance gains on other student with different encoders and decoders are also consistently achieved. As for PSPNet-MBV2, our method achieves a superior performance of 27.97%, surpassing the student, SKDS and IFVD by 4.82%, 3.18% and 2.64%. The gain on Deeplab-R18 with our CW is 2.48%, outperforming the SKDS and IFVD by 1.85% and 0.84%. Finally, the performance of Deeplab-MBV2 with our channel-wise distillation is increased from 24.98% to 29.18%, outperforming the SKDS and IFVD by 3.08% and 1.93% respectively.

S3. More visualization results of channel-wise distillation

We list the visualization results in Figure 7 to intuitively demonstrate that, the channel-wise distillation method (CW) outperforms the spatial distillation strategy

(attention transfer). Besides, to evaluate the effectiveness of the proposed channel-wise distillation, we visualize the channel-wise distribution of the student network under three paradigms, *i.e.*, original network, distilled by the attention transfer (AT) and channel-wise alignment respectively, in Figure 8.

S4. Optimization

For a fair comparison, in our experiments, we introduce the pixel-wise distillation and the holistic distillation as additional losses, which are used as a complement to the spatial proposed structural transfer method in [36, 45]. We also use them to align the score map. The loss of pixel-wise distillation is defined as follows,

$$\varphi_{pi}(q_i^s, q_i^t) = \frac{\sum_{i \in \mathcal{R}} \text{KL}(q_i^s \| q_i^t)}{W \times H} \quad (6)$$

where i is the index of all the pixels $\mathcal{R} = \{1, 2, \dots, W \times H\}$. W and H is the width and height of the score map. $q_i^s(t)$ denote the class probabilities of the i th pixel in score map from student (teacher) respectively. $\text{KL}(\cdot)$ is the Kullback-Leibler divergence.

Holistic distillation for segmentation leverages the adversarial learning to minimize the discrepancy of distribution between teacher’s score map S_t and student’s score map S_s , which is evaluated by the Wasserstein distance [22]:

$$\varphi_{ho}(S_s, S_t) = E_{Q^s \sim p_s(S^s)}[D(Q^s | I)] - E_{Q^t \sim p_t(S^t)}[D(Q^t | I)] \quad (7)$$

where $E[\cdot]$ denotes the expectation operator, I is the raw input image, and $D(\cdot)$ is used as a discriminator to transform the input Q to a holistic embedding score, where gradient penalty is ensured by lipschitz requirement and two self-attention modules are inserted between the last three layers to capture the structural information as in [36, 45]. For the proposed channel-aware fore/back-ground alignment method, the whole training object includes three components, *i.e.*, the original cross-entropy loss L_{ori} for segmentation, the pixel-wise distillation loss φ_{pi} , the holistic distillation loss φ_{ho} and the channel-aware fore/back-ground distillation loss φ_{cw} :

$$L = L_{ori} + \alpha_{pi} \cdot \varphi_{pi} - \alpha_{ho} \cdot \varphi_{ho} + \alpha_{cw} \cdot \varphi_{cw} \quad (8)$$

where α_{pi} , α_{ho} , α_{cw} are set as 10, 0.1 and 35 respectively. The training process is implemented by iterating the following two steps:

- **Training the student.** With the discriminator network and teacher network fixed, minimizing the summation of the original cross-entropy loss L_{ori} for segmentation, the pixel-wise distillation loss φ_{pi} , the holistic

distillation loss for student φ_{ho}^s and the channel-aware fore/back-ground distillation loss φ_{cw} :

$$L = L_{ori} + \alpha_{pi} \cdot \varphi_{pi} - \alpha_{ho} \cdot \varphi_{ho}^s + \alpha_{cw} \cdot \varphi_{cw} \quad (9)$$

where φ_{ho}^s is defined as follow:

$$\varphi_{ho}^s = E_{Q^s \sim p_s(S^s)}[D(Q^s | I)] \quad (10)$$

- **Training the discriminator.** We freeze the student network and teacher network, and minimize the φ_{ho} .

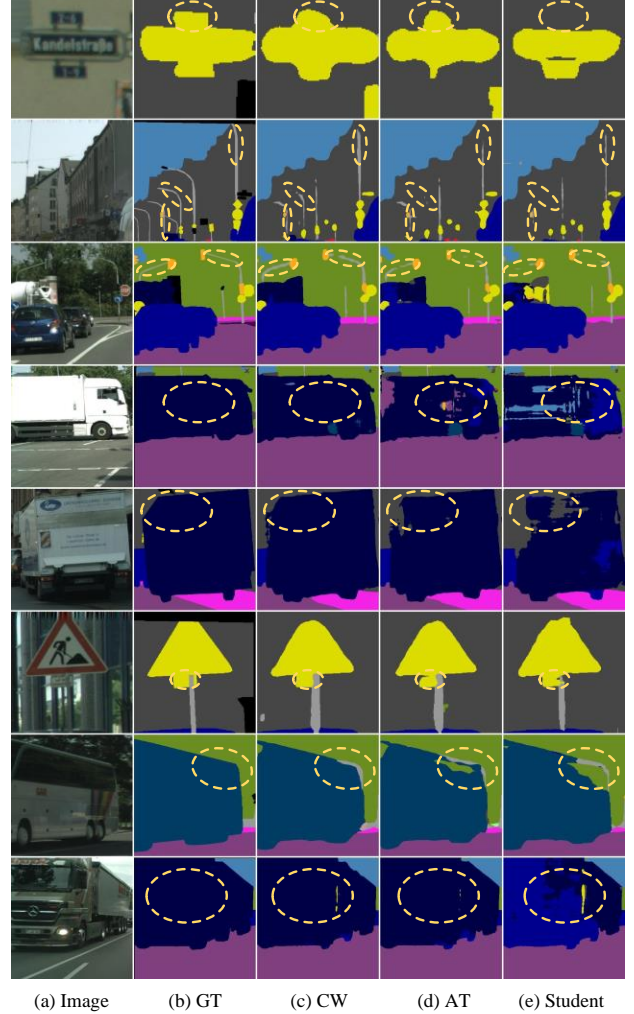


Figure 7 – Qualitative segmentation results on Cityscapes produced from PSPNet-R18: (a) raw images, (b) ground truth (GT), (c) channel-wise distillation (CW), (d) the spatial distillation schemes: attention transfer (AT), and (e) output of the original student model.

S5. Detection results

We also apply our channel-wise distillation method on the object detection task. The experiment are conducted

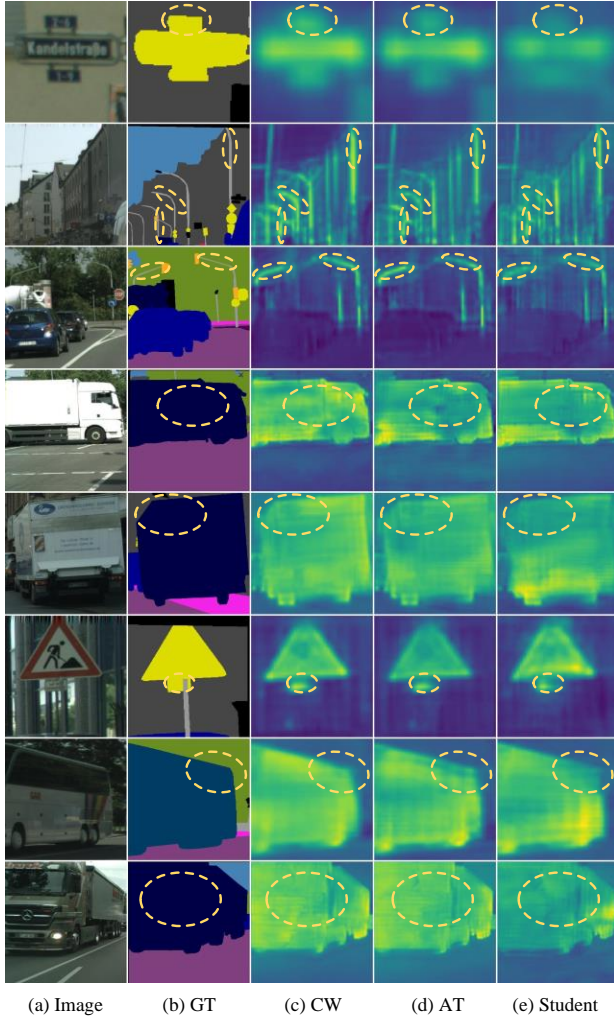


Figure 8 – The channel-wise fore/background distribution of the student under three paradigms. (a) raw images, (b) ground truth (GT), (c) channel-wise distillation (CW), (d) the spatial distillation schemes: attention transfer (AT), and (e) output of the original student model.

on MS COCO2017 (a large dataset that contains 80 categories with over 120k images). Multi student variants under different paradigm, *i.e.*, a two-stage anchor based method (Faster RCNN), a one-stage anchor based method (RetinaNet) and anchor-free method (RepPoints), are used to validate the efficiency of our method. To make a fair comparison, we conduct the experiment on the same teacher and student networks with the same hyper-parameters as in [54]. The only modification is that the feature alignment is changed to our channel-wise distillation.

Declaration of Conflicting Interests: Chunhua Shen and his employer received no financial support for the research, authorship, and/or publication of this article.

References

- [1] Paszke Adam, Chaurasia Abhishek, Kim Sangpil, and Culurciello Eugenio. Enet: A deep neural network architecture for real-time semantic segmentation. *IEEE Conf. Comput. Vis. Pattern Recog.*, 2016. 8
- [2] Romero Adriana, Ballas Nicolas, Ebrahimi Kahou Samira, Chassang Antoine, Gatta Carlo, and Bengio Yoshua. Fitnets: Hints for thin deep nets. *Int. Conf. Learn. Represent.*, 2015. 1, 3, 4, 5, 6
- [3] Sungsoo Ahn, Shell Xu Hu, Andreas Damianou, Neil D Lawrence, and Zhenwen Dai. Variational information distillation for knowledge transfer. In *IEEE Conf. Comput. Vis. Pattern Recog.*, pages 9163–9171, 2019. 1
- [4] Porrello Angelo, Bergamini Luca, and Calderara Simone. Robust re-identification by multiple views knowledge distillation. *Eur. Conf. Comput. Vis.*, 2020. 2
- [5] Jimmy Ba and Rich Caruana. Do deep nets really need to be deep? *Adv. Neural Inform. Process. Syst.*, 2014. 2
- [6] Jimmy Ba and Rich Caruana. Darkrank: Accelerating deep metric learning via cross sample similarities transfer. *AAAI Conf. Artificial Intelligence*, 2018. 2
- [7] Anil Bhattacharyya. On a measure of divergence between two statistical populations defined by their probability distributions. *Bull. Calcutta Math. Soc.*, 35:99–109, 1943. 5, 6
- [8] Yue Cao, Jiarui Xu, Stephen Lin, Fangyun Wei, and Han Hu. Gcnnet: Non-local networks meet squeeze-excitation networks and beyond. pages 0–0, 2019. 9
- [9] Guobin Chen, Wongun Choi, Yu Xiang, Han Tony, and Manmohan Chandraker. Learning efficient object detection models with knowledge distillation. *Adv. Neural Inform. Process. Syst.*, 2017. 2
- [10] Guobin Chen, Wongun Choi, Xiang Yu, Tony Han, and Manmohan Chandraker. Learning efficient object detection models with knowledge distillation. In *Adv. Neural Inform. Process. Syst.*, pages 742–751, 2017. 12
- [11] Hanting Chen, Yunhe Wang, Han Shu, Changyuan Wen, Chunjing Xu, Boxin Shi, Chao Xu, and Chang Xu. Distilling portable generative adversarial networks for image translation. In *AAAI Conf. Artificial Intelligence*, 2020. 2
- [12] Liang-Chieh Chen, George Papandreou, Florian Schroff, and Hartwig Adam. Rethinking atrous convolution for semantic image segmentation. *IEEE Conf. Comput. Vis. Pattern Recog.*, 2017. 8, 9
- [13] Wuyang Chen, Xinyu Gong, Xianming Liu, Qian Zhang, Yuan Li, and Zhangyang Wang. Fasterseg: Searching for faster real-time semantic segmentation. *Int. Conf. Learn. Represent.*, 2020. 4, 5, 6
- [14] Xinghao Chen, Yiman Zhang, Yunhe Wang, Han Shu, Chunjing Xu, and Chang Xu. Optical flow distillation: Towards efficient and stable video style transfer. In *Eur. Conf. Comput. Vis.*, 2020. 2
- [15] Yuhua Chen, Wen Li, and Gool Luc. Road: Reality oriented adaptation for semantic segmentation of urban scenes. *IEEE Conf. Comput. Vis. Pattern Recog.*, 2018. 2
- [16] Marius Cordts, Mohamed Omran, Sebastian Ramos, Timo Rehfeld, Markus Enzweiler, Rodrigo Benenson, Uwe

Model		Backbone	AP	AP ₅₀	AP ₇₅	AP _S	AP _M	AP _L	FPS	Params (M)
Two-stage anchor based	Faster RCNN	R50	38.4	59.0	42.0	21.5	42.1	50.3	18.1	43.57
	+Chen et al.'s method [10]		38.7	59.0	42.1	22.0	41.9	51.0	18.1	43.57
	+Wang et al.'s [44]		39.1	59.8	42.8	22.2	42.9	51.1	18.1	43.57
	+Heo et al.'s [25]		38.9	60.1	42.6	21.8	42.7	50.7	18.1	43.57
	+Zhang et al.'s [54]		41.5	62.2	45.1	23.5	45.0	55.3	18.1	43.57
	+Our Method		41.7	62.0	45.5	23.3	45.5	55.5	18.1	43.57
One-stage anchor based	RetinaNet	R50	37.4	56.7	39.6	20.0	40.7	49.7	20.0	36.19
	+Heo et al. [25]		37.8	58.3	41.1	21.6	41.2	48.3	20.0	36.19
	+Zhang et al. [54]		39.6	58.8	42.1	22.7	43.3	52.5	20.0	36.19
	+Our Method		40.8	60.4	43.4	22.7	44.5	55.3	20.0	36.19
Anchor free	RepPoints	R50	38.6	59.6	41.6	22.5	42.2	50.4	18.2	36.62
	+Zhang et al. [54]		40.6	61.7	43.8	23.4	44.6	53.0	18.2	36.62
	+Our Method		42.0	63.0	45.3	24.1	46.1	55.0	18.2	36.62

Table 9 – Comparison between our methods and other distillation methods on object detection. Our method consistently beats other distillation methods.

- Franke, Stefan Roth, and Bernt Schiele. The cityscapes dataset for semantic urban scene understanding. *IEEE Conf. Comput. Vis. Pattern Recog.*, 2016. 4
- [17] Jiajun Deng, Yingwei Pan, Ting Yao, Wengang Zhou, Houqiang Li, and Tao Mei. Relation distillation networks for video object detection. *Int. Conf. Comput. Vis.*, 2019. 2
- [18] Romera Eduardo, Álvarez José M, Bergasa Luis M, and Arroyo Roberto. Erfnet: Efficient residual factorized convnet for real-time semantic segmentation. *IEEE Trans. Intell. Transportation Syst.*, 2017. 8
- [19] Mark Everingham, Luc Van Gool, Christopher K. I. Williams, John Winn, and Andrew Zisserman. The pascal visual object classes (voc) challenge. *Int. J. Comput. Vis.*, 2010. 4
- [20] Jie Fu, Xue Geng, Zhijian Duan, Bohan Zhuang, Xingdi Yuan, Adam Trischler, Jie Lin, Chris Pal, and Hao Dong. Role-wise data augmentation for knowledge distillation. *Int. Conf. Learn. Represent.*, 2020. 2
- [21] Yushuo Guan, Pengyu Zhao, Bingxuan Wang, Yuanxing Zhang, Cong Yao, Kaigui Bian, and Jian Tang. Differentiable feature aggregation search for knowledge distillation. In *Eur. Conf. Comput. Vis.*, 2020. 2
- [22] Ishaan Gulrajani, Faruk Ahmed, Martin Arjovsky, Vincent Dumoulin, and Aaron C Courville. Improved training of wasserstein gans. In *Adv. Neural Inform. Process. Syst.*, pages 5767–5777, 2017. 10
- [23] Kaiming He, Xiangyu Zhang, Shaoqing Ren, and Jian Sun. Deep residual learning for image recognition. *IEEE Conf. Comput. Vis. Pattern Recog.*, 2016. 8
- [24] Tong He, Chunhua Shen, Tian Zhi, Dong Gong, Changming Sun, and Youliang Yan. Knowledge adaptation for efficient semantic segmentation. *IEEE Conf. Comput. Vis. Pattern Recog.*, 2019. 2, 3, 4, 5, 6
- [25] Byeongho Heo, Jeessoo Kim, Sangdoo Yun, Hyojin Park, Nojun Kwak, and JinYoung. Choi. A comprehensive overhaul of feature distillation. In *Int. Conf. Comput. Vis.*, pages 1921–19302, 2019. 12
- [26] Jain Himalaya, Gidaris Spyros, Komodakis Nikos, Pérez Patrick, and Cord Matthieu. Quest: Quantized embedding space for transferring knowledge. *IEEE Conf. Comput. Vis. Pattern Recog.*, 2020. 1
- [27] Geoffrey Hinton, Oriol Vinyals, and Jeff Dean. Distilling the knowledge in a neural network. *Adv. Neural Inform. Process. Syst.*, 2014. 1, 2
- [28] Geoffrey E. Hinton, Oriol Vinyals, and Jeffrey Dean. Distilling the knowledge in a neural network. *arXiv*, abs/1503.02531, 2015. 3
- [29] Yuenan Hou, Zheng Ma, Chunxiao Liu, and Chen Change Loy. Learning lightweight lane detection cnns by self attention distillation. *Int. Conf. Comput. Vis.*, 2019. 2
- [30] Yuenan Hou, Zheng Ma, Chunxiao Liu, Tak-Wai Hui, and Chen Change Loy. Inter-region affinity distillation for road marking segmentation. In *IEEE Conf. Comput. Vis. Pattern Recog.*, pages 12486–12495, 2020. 2, 7
- [31] Yuge Huang, Pengcheng Shen, Ying Tai, Shaoxin Li, Xiaoming Liu, Jilin Li, Feiyue Huang, and Rongrong Ji. Improving face recognition from hard samples via distribution distillation loss. In *Eur. Conf. Comput. Vis.*, 2020. 2
- [32] Long Jonathan, Shelhamer Evan, and Darrell Trevor. Fully convolutional networks for semantic segmentation. *IEEE Conf. Comput. Vis. Pattern Recog.*, 2015. 8, 9
- [33] Muyang Li, Ji Lin, Yaoyao Ding, Zhijian Liu, Jun-Yan Zhu, and Song Han. Gan compression: Efficient architectures for interactive conditional gans. In *IEEE Conf. Comput. Vis. Pattern Recog.*, 2020. 2
- [34] Quanquan Li, Shengying Jin, and Junjie Yan. Mimicking very efficient network for object detection. *IEEE Conf. Comput. Vis. Pattern Recog.*, 2017. 3, 4, 5, 6
- [35] Guosheng Lin, Anton Milan, Chunhua Shen, and Ian Reid. Refinenet: Multi-path refinement networks for high-resolution semantic segmentation. *IEEE Conf. Comput. Vis. Pattern Recog.*, 2017. 8
- [36] Yifan Liu, Ke Chen, Chris Liu, Zengchang Qin, Zhenbo Luo, and Jingdong Wang. Structured knowledge distillation for semantic segmentation. *IEEE Conf. Comput. Vis. Pattern Recog.*, 2019. 2, 3, 4, 5, 6, 8, 9, 10
- [37] Yifan Liu, Changyong Shu, Jingdong Wang, and Chunhua Shen. Structured knowledge distillation for dense prediction.

- IEEE Trans. Pattern Anal. Mach. Intell.*, 2019. 2, 3, 4, 5, 6, 7, 8
- [38] Phuong Mary and Christoph H. Lampert. Distillation-based training for multi-exit architectures. *Int. Conf. Comput. Vis.*, 2019. 1
- [39] Wonpyo Park, Dongju Kim, Yan Lu, and Minsu Cho. Relational knowledge distillation. In *IEEE Conf. Comput. Vis. Pattern Recog.*, pages 3967–3976, 2019. 2
- [40] Mehta Sachin, Rastegari Mohammad, Caspi Anat, Shapiro Linda, and Hajishirzi Hannaneh. Espnet: Efficient spatial pyramid of dilated convolutions for semantic segmentation. *Eur. Conf. Comput. Vis.*, 2018. 8
- [41] Mark Sandler, Andrew Howard, Menglong Zhu, Andrey Zhmoginov, and Liang-Chieh Chen. Mobilenetv2: Inverted residuals and linear bottlenecks. *IEEE Conf. Comput. Vis. Pattern Recog.*, 2018. 8
- [42] Tao, Li Wang, Xiaopeng Yuan, Jiashi Zhang, and Feng. Distilling object detectors with fine-grained feature imitation. *IEEE Conf. Comput. Vis. Pattern Recog.*, 2019. 2
- [43] Guo-Hua Wang, Yifan Ge, and Jianxin Wu. In defense of feature mimicking for knowledge distillation. *arXiv preprint arXiv:2011.01424*, 2020. 4
- [44] Tao Wang, Li Yuan, Xiaopeng Zhang, and Jiashi. Feng. Distilling object detectors with fine-grained feature imitation. In *IEEE Conf. Comput. Vis. Pattern Recog.*, pages 4933–4942, 2019. 12
- [45] Yukang Wang, Zhou Wei, Jiang Tao, Bai Xiang, and Yongchao Xu. Intra-class feature variation distillation for semantic segmentation. *Eur. Conf. Comput. Vis.*, 2020. 2, 3, 4, 5, 6, 8, 9, 10
- [46] Ancong Wu, Wei-Shi Zheng, Xiaowei Guo, and Jian-Huang Lai. Distilled person re-identification: Towards a more scalable system. In *IEEE Conf. Comput. Vis. Pattern Recog.*, 2019. 2
- [47] Jiafeng Xie, Bing Shuai, JianFang Hu, Jingyang Lin, and WeiShi Zheng. Improving fast segmentation with teacher-student learning. *Brit. Mach. Vis. Conf.*, 2018. 2, 3, 4, 5, 6
- [48] Qizhe Xie, Minh-Thang Luong, Eduard Hovy, and Quoc V. Le. Self-training with noisy student improves imagenet classification. In *IEEE Conf. Comput. Vis. Pattern Recog.*, pages 3967–3976, 2019. 2
- [49] Guodong Xu, Ziwei Liu, Xiaoxiao Li, and Chen Change Loy. Knowledge distillation meets self-supervision. In *Eur. Conf. Comput. Vis.*, 2020. 2
- [50] Li Yuan, Francis EH Tay, Guilin Li, Tao Wang, and Jiashi Feng. Revisiting knowledge distillation via label smoothing regularization. In *IEEE Conf. Comput. Vis. Pattern Recog.*, pages 3903–3911, 2020. 2
- [51] Yuhui Yuan, Xilin Chen, and Jingdong Wang. Object-contextual representations for semantic segmentation. 2020. 9
- [52] Yuhui Yuan and Jingdong Wang. Ocnet: Object context network for scene parsing. *arXiv preprint arXiv:1809.00916*, 2018. 8
- [53] Sergey Zagoruyko and Nikos Komodakis. Paying more attention to attention: Improving the performance of convolutional neural networks via attention transfer. *Int. Conf. Learn. Represent.*, 2017. 3, 4, 5, 6
- [54] Linfeng Zhang and Kaisheng. Ma. Improve object detection with feature-based knowledge distillation: Towards accurate and efficient detectors. In *Int. Conf. Learn. Represent.*, 2021. 11, 12
- [55] Ying Zhang, Tao Xiang, Timothy M Hospedales, and Huchuan Lu. Deep mutual learning. *IEEE Conf. Comput. Vis. Pattern Recog.*, 2018. 1
- [56] Zizhao Zhang, Han Zhang, Serkan O Arik, Honglak Lee, and Tomas Pfister. Distilling effective supervision from severe label noise. In *IEEE Conf. Comput. Vis. Pattern Recog.*, 2020. 2
- [57] Hengshuang Zhao, Xiaojuan Qi, Xiaoyong Shen, Jianping Shi, and Jiaya Jia. Icnnet for real-time semantic segmentation on high-resolution images. *Eur. Conf. Comput. Vis.*, 2018. 8
- [58] Hengshuang Zhao, Yi Zhang, Shu Liu, Jianping Shi, Chen Change Loy, Dahua Lin, and Jiaya Jia. Psanet: Point-wise spatial attention network for scene parsing. In *Eur. Conf. Comput. Vis.*, pages 267–283, 2018. 9
- [59] Hengshuang Zhao, Jianping Shi, Xiaojuan Qi, Xiaogang Wang, and Jiaya Jia. Pyramid scene parsing network. *IEEE Conf. Comput. Vis. Pattern Recog.*, 2020. 8, 9
- [60] Bolei Zhou, Hang Zhao, Xavier Puig, Sanja Fidler, Adela Barriuso, and Antonio. Torralba. Scene parsing through ade20k dataset. *IEEE Conf. Comput. Vis. Pattern Recog.*, 2017. 4
- [61] Zaida Zhou, Zhuge Chaoran, Xinwei Guan, and Wen Liu. Channel distillation: Channel-wise attention for knowledge distillation. *arXiv*: abs/2006.01683, 2020. 2, 3
- [62] Zhen Zhu, Mengde Xu, Song Bai, Tengting Huang, and Xiang Bai. Asymmetric non-local neural networks for semantic segmentation. *Int. Conf. Comput. Vis.*, 2019. 9